Mathematical Biosciences and Engineering

http://www.aimspress.com/journal/mbe

MBE, 21(1): 832–860.
DOI: 10.3934/mbe.2024035
Received: 10 October 2023
Revised: 03 December 2023
Accepted: 10 December 2023
Published: 20 December 2023

Research article

Dynamical behaviours of discrete amensalism system with fear effects on first species

Qianqian Li[1], Ankur Jyoti Kashyap[2], Qun Zhu[1] and Fengde Chen[1,*]

[1] School of Mathematics and Statistics, Fuzhou University, Fuzhou 350108, China

[2] Department of Mathematics, Girijananda Chowdhury University, Assam, India

* **Correspondence:** Email: fdchen@fzu.edu.cn.

Abstract: Amensalism, a rare yet impactful symbiotic relationship in ecological systems, is the focus of this study. We examine a discrete-time amensalism system by incorporating the fear effect on the first species. We identify the plausible equilibrium points and analyze their local stability conditions. The global attractivity of the positive equilibrium, E^*, and the boundary equilibrium, E_1, are analyzed by exploring threshold conditions linked to the level of fear. Additionally, we analyze transcritical bifurcations and flip bifurcations exhibited by the boundary equilibrium points analytically. Considering some biologically feasible parameter values, we conduct extensive numerical simulations. From numerical simulations, it is observed that the level of fear has a stabilizing effect on the system dynamics when it increases. It eventually accelerates the extinction process for the first species as the level of fear continues to increase. These findings highlight the complex interplay between external factors and intrinsic system dynamics, enriching potential mechanisms for driving species changes and extinction events.

Keywords: fear effect; amensalism; global attractivity; chaos control; transcritical bifurcation; flip bifurcation

1. Introduction

Symbiotic relationships play a crucial role in the study of ecological systems and have gained substantial attention among evolutionary biologists for their frequent involvement in the coevolutionary dynamics between interacting organisms. In addition to well-known symbiotic relationships like mutualism, competition and predator/prey interactions, there are three other types, i.e., commensalism, amensalism and synnecrosis, that have received comparatively less attention from researchers. Amensalism, receiving less attention than commensalism, involves one species adversely affecting another's fitness without gaining any apparent benefit [1] For instance, Xi et al. [2] noted that grassland cater-

pillars will trigger a death-feigning anti-predator response if grasshoppers suddenly appear. Moreover, by leaping to seek food, the grasshopper may negatively affect the foraging efficiency of the caterpillars, but the behavior of caterpillars has no effect on the grasshopper. Therefore, the two species form an amensalism relationship. The interaction of ibex and weevils feeding on the same type of shrub serves as another illustration of amensalism. Although the presence of the weevil has minimal impact on food availability, the presence of ibex significantly reduces weevil populations. Ibex consume substantial amounts of plant matter, inadvertently ingesting the weevils along with it [3]. According to Veiga et al. [4] the relationships witnessed between honey bees (*Apis mellifera*) and wasps in the tropical ecosystems of East Africa could be described by amensalism concerning nesting spaces. The experiment's results revealed that wasps refrained from using nest boxes that had been inhabited by bees in the prior breeding season. In contrast, honeybees displayed a tendency to take over these nest boxes, regardless of whether they were previously occupied by wasps. This behavior showcases a clear instance of amensalism, as there was no recorded occurrence of wasps occupying a nest box previously utilized by bees. For a deeper ecological context regarding species amensalism, refer to [3, 5–8] and the related references within those sources.

Although scientists and researchers have extensively investigated amensalism in ecological systems in recent decades, the first mathematical model was put forward by Sun in 2003 [9]. In 2008, Zhu et al. [10] employed the method of vector field analysis to study the following model:

$$\begin{cases} \dfrac{dx}{dt} = x\,(a_1 - b_1 x - c_1 y)\,, \\ \dfrac{dy}{dt} = y\,(a_2 - c_2 y)\,, \end{cases} \tag{1.1}$$

where x and y represent the density of the first and second species at time t, respectively, a_1 and b_1 stand for the intrinsic growth rates and the intensity of competition of x, a_2 and c_2 stand for the intrinsic growth rates and the intensity of competition of y. Additionally, c_1 represents the strength of the interspecific competition, indicating how much impact the second species has on the first species. By analyzing the equilibrium points in system (1.1), they obtained the following result:

Theorem A (1) If $\frac{a_1}{c_1} < \frac{a_2}{c_2}$, then the boundary fixed points $B(0, \frac{a_2}{c_2})$ is globally stable.
(2) If $\frac{a_1}{c_1} > \frac{a_2}{c_2}$, then the unique positive fixed point $A(\frac{a_1c_2-c_1a_2}{b_1c_2}, \frac{a_2}{c_2})$ is globally stable.

The model (1.1) exhibits simple dynamical behavior as the Theorem A indicates that the system does not generate bifurcation. In recent years, researchers have extensively studied the dynamical behaviors of the amensalism model (1.1) in different scenarios. Several mathematical models have been explored, considering the well-known Allee effect in [11–15]. For instance, Wei et al. [11] proposed an amensalism model with a weak Allee effect and observed saddle-node bifurcations. Luo et al. [12] presented the global dynamics of a two-species Holling-II amensalism system with a nonlinear growth rate by incorporating the Allee effect on the first species. Similarly, some interesting works using non-monotonic functional responses have been presented in [6, 16, 18]. Amensalism relationships among different species have also been incorporated into the study of harvesting models [19, 20]. Under the Michaelis-Menten type harvesting in the first species, Liu et al. [19] investigated the complex dynamics of an amensalism system. Zhao et al. [20] found that incorporating Menten-type harvesting in the second species within the amensalism system leads to notably richer dynamics. These dynamics include scenarios where the extinction of the first species persists or where the approach toward the steady-state occurs at a slower rate. Similar to the above, amensalism models incorporating prey refuge

have emerged as a prominent area of research [19, 21, 22, 24].

In ecological systems, direct killing in the predation process significantly influences the common symbiosis relationships, i.e., mutualisms, competition and predator/prey interactions. Besides direct killing, the psychological fear induced in the prey due to predation risk also indirectly impacts the breeding rate of the prey. This indirect effect, termed the fear effect, exerts a substantial impact throughout the prey's life cycle, amplifying the complexity of their ecological dynamics. In their experiment involving song sparrows, Zanette et al. [25] observed a 40% reduction in the breeding rate due to the induced fear of predation risk. In another independent study, Elliott et al. [26] reported that Drosophila melanogaster exhibits anti-predator behaviors upon exposure to Mantid odor, displaying reduced activity across both breeding and non-breeding seasons. Meanwhile, Wang et al. [27] presented a mathematical model for prey-predator dynamics, incorporating the fear risk. They disclosed that heightened fear levels might stabilize the ecosystem by preventing the occurrence of periodic oscillations in the population. For more information about predator-prey models with fear effects, see [28–30] and references cited therein. The fear effect is not limited to only common symbiosis relationships like mutualism, competition and predator/prey interactions. It has also been observed in commensalism and amensalism types of symbiosis. For example, Xi et al. [2] studied the number of cocoons formed by grassland caterpillars in the presence or absence of grasshoppers and obtained Figure 1. From Figure 1, it can be clearly observed that the fear of grasshoppers by caterpillars can lead to a decline in species numbers. Ogada [31] have highlighted that the presence of large herbivorous mammals in African savanna habitats has resulted in a reduction of the canopy area of trees, as well as a decrease in grass cover by 8% and forb cover by 33%. However, the canopy serves as a crucial habitat and food source for birds in this particular East African savanna ecosystem. Thus, the sizable herbivore has exerted a significant influence on avian behavior and growth, particularly in relation to foraging habits, rates of maturation, chances of survival, reproductive capacity and dietary resources. As a result, the overall diversity of bird species has experienced a decline of approximately 30%. This decline may be interpreted as the fear induced by large herbivores in the East African savanna ecosystem, resulting in reduced avian birth rates. Consequently, developing models that can effectively explain this phenomenon is imperative. However, no scholarly investigations have taken into account the impact of the fear effect on the amensalism system.

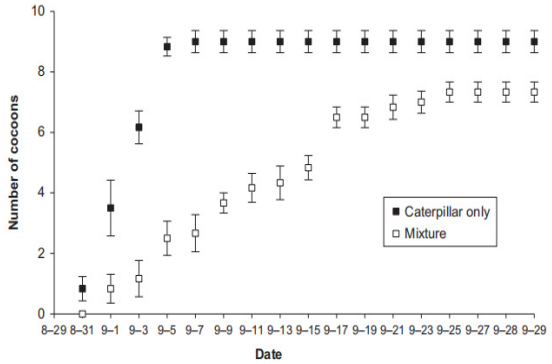

Figure 1. The number of cocoons formed by grassland caterpillars in the presence or absence of grasshoppers.

Recently, discrete-time models have attracted considerable attention due to their rich and complex

dynamic behaviors and have been explored extensively [18, 30, 32]. However, there needs to be more emphasis on investigating discrete-time amensalism systems. In 2022, Zhou et al. [21] investigated the following discrete amensalism systems:

$$\begin{cases} x_{n+1} = x_n \exp(\alpha - \beta x_n - c y_n), \\ y_{n+1} = y_n \exp(\gamma - \delta y_n). \end{cases} \tag{1.2}$$

They studied the stability and attractivity of the equilibrium point of system (1.2) and obtained the following results:

Theorem B (1) If $0 < \alpha \leq 2$, $0 < c < \frac{\delta\alpha}{\gamma}$, $0 < \gamma < 2$ or $\alpha > 2$, $\frac{\delta(\alpha-2)}{\gamma} < c < \frac{\delta\alpha}{\gamma}$, $0 < \gamma < 2$, then the positive equilibrium point $E_3^*(x_3^*, \frac{\gamma}{\delta})$ is local stability.
(2) If $0 < \gamma < 2$, $0 < \alpha - \frac{c\gamma}{\delta} < \ln 2 + 1$, then the positive equilibrium point $E_3^*(x_3^*, \frac{\gamma}{\delta})$ is globally attractive.

Obviously, system (1.2) is the discrete form of model (1.1). In system (1.1), according to Theorem A (2), when a positive equilibrium point exists, it is global stability. This also implied that no matter what the initial conditions are, the solution will eventually converge to the positive equilibrium point. While for discrete system (1.2), Theorem B shows that the conclusion of the stability of the positive equilibrium point can only be obtained under stricter conditions than Theorem A. Additionally, model (1.2) undergoes flip bifurcation at the boundary equilibrium points E_1, E_2 and the positive equilibrium point E_3^* [21]. This is a dynamic phenomenon that does not exist in the continuous system (1.1), Hence, the investigation of discrete models is highly valuable due to their propensity for exhibiting intricate dynamic phenomena that surpass those observed in continuous models.

Subsequently, Zhou et al. [32] investigated a discrete amensalism system with the Beddington-DeAngelies functional response and Allee effect, and they found that the Allee effect causes the system to take longer trajectories to reach its stable steady-state solution. So far, to the best of our knowledge, there has been no research conducted on the discrete amensalism system with the fear effect by researchers.

Motivated by prior research, we assume that the birth rate of the first species will be reduced by the fear of the second species. We multiply the birth rate of the first species by a decreasing function $G(k, y)$ related to the size of the second species. Based on observations in the biological world, the fear function $G(k, y)$ proposed by Wang et al. [27] must satisfy the following requirements:

$$G(0, y) = 1, G(k, 0) = 1, \lim_{y\to\infty} G(k, y) = 0,$$

$$\lim_{k\to\infty} G(k, y) = 0, \frac{\partial G(k, y)}{\partial k} < 0, \frac{\partial G(k, y)}{\partial y} < 0,$$

where k represents the level of fear and y is the species density. Note that $G(k, y) = 1/(1 + ky)$ meets the above requirements and $1/(1 + ky)$ is now widely applied in [33–35].

Accordingly, on the basis of system (1.1), considering the above assumption, we introduce the fear effect to the first species, resulting in the formulation of the following amensalism model:

$$\begin{cases} \dfrac{dx}{dt} = x\left(\dfrac{e_1}{1 + k_1 y} - e_2 - b_1 x - c_1 y\right), \\ \dfrac{dy}{dt} = y(a_2 - c_2 y), \end{cases} \tag{1.3}$$

where e_1 and e_2 represent the birth and death rates of the first species and $1/(1 + ky)$ represents the fear effect function. It is to be noted that without the fear effect ($k = 0$), the above model (1.3) will degenerate to the amensalism model (1.1). For the convenience of analysis, with the transformation $x = \bar{x}/b_1$, $y = \bar{y}/c_2$, $t = \bar{t}$, after dropping the bars, system (1.3) becomes

$$\begin{cases} \dfrac{dx}{dt} = x\left(\dfrac{e_1}{1+ky} - e_2 - x - cy\right), \\ \dfrac{dy}{dt} = y\,(a_2 - y)\,, \end{cases} \tag{1.4}$$

where $k = k_1/c_2$ and $c = c_1/c_2$. The numerical simulations in [36] show that when the step size gets bigger in Euler's scheme, both period-doubling and Neimark-Sacker bifurcation happen. This means that the numerical approach for discretization is not accurate. In order to address this shortcoming, the method of piecewise constant arguments was established. Based on the findings in [37,38], the method of piecewise constant arguments is indeed a preferable solution for the discretization of continuous models. Hence, using the method of piecewise constant arguments proposed by Jiang and Rogers [39], similar to the modeling method in [32], we can obtain the following discrete-time model:

$$\begin{cases} x_{n+1} = x_n \exp\left(\dfrac{e_1}{1+ky_n} - e_2 - x_n - cy_n\right), \\ y_{n+1} = y_n \exp\left(a_2 - y_n\right). \end{cases} \tag{1.5}$$

Obviously, the initial conditions (x_0, y_0) for (1.5) are in $\mathbb{R}^2_+$. In a discrete amensalism ecological model with the fear effect, what kind of dynamical behavior does it exhibit? Does the stability of the equilibrium point change compared to a continuous system (1.1)? Does a new bifurcation happen compared to a discrete system (1.2)? What effects do fear effects have on the system? We will conduct a detailed investigation to answer these questions.

The layout of the paper is as follows: In Section 2, we analyze the relevant properties of the fixed points. Section 3 investigates bifurcation phenomena and considers the chaos control method. Then, in Section 4, we use numerical simulations to validate the feasibility of the obtained results. Finally, a brief discussion is provided at the end of the paper.

2. Analysis of fixed points

2.1. The existence of equilibria

Note that fixed points are determined by the following system of equations:

$$\begin{cases} x = x\exp\left(\frac{e_1}{1+ky} - e_2 - x - cy\right), \\ y = y\exp\left(a_2 - y\right). \end{cases} \tag{2.1}$$

Obviously, system (1.5) always has four fixed points: $E_0(0,0)$, $E_1(0,a_2)$, $E_2(e_1 - e_2, 0)$ and $E^*((e_1 - e_2 - ke_2a_2 - ka_2^2c - a_2c)/(1 + ka_2), a_2)$. The fixed points E_2 and E^* are non-negative if $e_2 < e_1$ and $e_1 > (a_2k + 1)(a_2c + e_2)$ are satisfied, respectively. There are two fixed points in region A of Figure 2(a): E_0 and E_1. There are three fixed points in region B: E_0, E_1 and E_2. There are four fixed points in region C: E_0, E_1, E_2 and E^*.

2.2. The local stability of equilibria

The Jacobian matrix of system (2.1) is calculated as follows:

$$J(x,y)=\begin{pmatrix} (1-x)M & -x\Big(\dfrac{e_1k}{(1+ky)^2}+c\Big)M \\ 0 & (1-y)N \end{pmatrix}, \tag{2.2}$$

where $M=\exp(e_1/(1+ky)-e_2-x-cy)$ and $N=\exp(a_2-y)$.

Next, we analyze the local stability of the equilibria according to the above Jacobian matrix.

Theorem 2.1. *$E_0(0,0)$ is*

1) a source if $0<e_2<e_1$;

2) a saddle if $0<e_1<e_2$;

3) non-hyperbolic if $e_1=e_2$.

Proof. For the equilibrium $E_0(0,0)$, the Jacobian matrix is

$$J(E_0)=\begin{pmatrix} \exp(e_1-e_2) & 0 \\ 0 & \exp(a_2) \end{pmatrix},$$

with eigenvalues $\lambda_1=\exp(e_1-e_2)>0$ and $\lambda_2=\exp(a_2)>1$. Thus, $E_0(0,0)$ is a source if $0<e_2<e_1$, a saddle if $0<e_1<e_2$ and non-hyperbolic if $e_1=e_2$. The proof is completed.

Theorem 2.2. *The local stability of $E_1(0,a_2)$ is described below:*

1) a sink if $0<e_1<(a_2k+1)(a_2c+e_2)$ and $0<a_2<2$;

2) a source if $e_1>(a_2k+1)(a_2c+e_2)$ and $a_2>2$;

3) non-hyperbolic if $e_1=(a_2k+1)(a_2c+e_2)$ or $a_2=2$;

4) a saddle if one of the conditions holds:

(a) $0<e_1<(a_2k+1)(a_2c+e_2)$ and $a_2>2$;

(b) $e_1>(a_2k+1)(a_2c+e_2)$ and $0<a_2<2$.

Proof. The Jacobian matrix of system (2.1) at $E_1(0,a_2)$ is given by

$$J(E_1)=\begin{pmatrix} \exp\big(\frac{e_1}{1+ka_2}-e_2-ca_2\big) & 0 \\ 0 & 1-a_2 \end{pmatrix}.$$

Consequently, two eigenvalues are $\lambda_1=\exp(e_1/(1+ka_2)-e_2-ca_2)>0$ and $\lambda_2=1-a_2<1$. Hence, if $0<e_1<(a_2k+1)(a_2c+e_2)$ and $0<a_2<2$, then we have $0<\lambda_1<1$ and $|\lambda_2|<1$. Therefore, $E_1(0,a_2)$ is a sink. The proofs of (2–4) are similar to (1) and are omitted here. The topological classification of E_1 is presented in Figure 2(b).

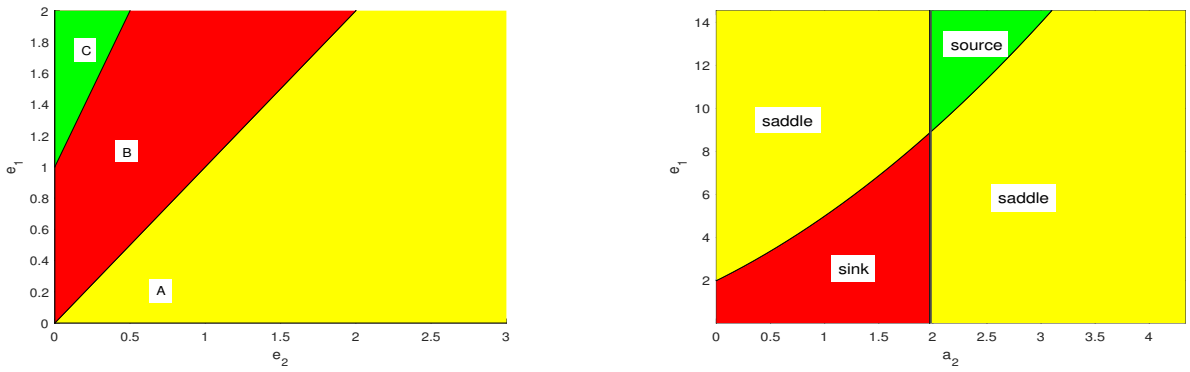

(a) (b)

Figure 2. (a) Classification diagram of the existence of equilibrium points with $c = 0.5$, $a_2 = 1$, $k = 1$, $e_2 \in (0, 3)$, $e_1 \in (0, 2)$. (b) topological classification of $a_2 - e_1$ plane at E_1 with $k = 1$, $c = 0.5$, $e_2 = 2$, $a_2 \in (0, 5)$, $e_1 \in (0, 14)$.

Theorem 2.3. *$E_2(e_1 - e_2, 0)$ is*

1) a source if $e_1 > e_2 + 2$;

2) a saddle if $0 < e_1 < 2 + e_2$;

3) non-hyperbolic if $e_1 - e_2 = 2$.

Proof. For the equilibrium $E_2(e_1 - e_2, 0)$, the Jacobian matrix is

$$J(E_2) = \begin{pmatrix} 1 - e_1 + e_2 & e_1 - e_2(-e_1k - c) \\ 0 & \exp(a_2) \end{pmatrix}.$$

Obviously, the two eigenvalues are $\lambda_1 = 1 - e_1 + e_2 = 1 - (e_1 - e_2) < 1$ and $\lambda_2 = \exp(a_2) > 1$. If $e_1 - e_2 > 2$, i.e., $\lambda_1 < -1$, then $|\lambda_1| > 1$ and $|\lambda_2| > 1$, implying that $E_2(e_1 - e_2, 0)$ is a source. Therefore, (1) holds. The proof processes of (2) and (3) are similar, we omit the details here. Thus, E_2 is always unstable. This completes the proof.

For $E^*(x^*, a_2)$, the Jacobian matrix is as follow:

$$J(E^*) = \begin{pmatrix} 1 - x^* & x^*\left(\frac{e_1k}{(1+ka_2)^2} + c\right) \\ 0 & 1 - a_2 \end{pmatrix},$$

where $\lambda_1 = 1 - x^* = 1 - (e_1 - (1 + a_2k)(e_2 + ca_2))/(1 + ka_2) < 1$ and $\lambda_2 = 1 - a_2 < 1$. Note that when $0 < c < (e_1 - e_2(1 + ka_2))/(1 + ka_2)a_2 \triangleq \tilde{c}$ and $0 < e_2 < e_1/(1 + ka_2) - 2 \triangleq e_2^{**}$. In addition, we can verify $c_1 < \tilde{c}$. Then,

$$1 - \frac{e_1 - (1 + a_2k)(e_2 + ca_2)}{1 + ka_2} \begin{cases} < -1 & \text{if } 0 < c < c_1, \\ = -1 & \text{if } c = c_1, \\ \in (-1, 1) & \text{if } c_1 < c < \tilde{c}, \end{cases}$$

where $c_1 = (e_1 - (2 + e_2)(1 + ka_2))/(1 + ka_2)a_2$. Moreover, if $e_2^{**} < e_2 < e_1/(1 + ka_2)$ and $0 < c < \tilde{c}$, then $1 - x^* \in (-1, 1)$. Therefore, the following result can be obtained immediately.

Theorem 2.4. *Suppose that* $0 < c < \tilde{c}$. *Then, the topological classifications of the unique positive fixed point* $E^*(x^*, a_2)$ *is given by Table 1.*

Table 1. Topological types of the fixed point $E^*(x^*, a_2)$.

Conditions			**Case**
$e_2^{**} < e_2 < \frac{e_1}{1+ka_2}$	$0 < c < \tilde{c}$	$0 < a_2 < 2$	sink
		$a_2 > 2$	saddle
		$a_2 = 2$	non-hyperbolic
$0 < e_2 < e_2^{**}$	$0 < c < c_1$	$0 < a_2 < 2$	saddle
		$a_2 > 2$	source
		$a_2 = 2$	non-hyperbolic
	$c = c_1$	$0 < a_2 < 2$	non-hyperbolic
		$a_2 > 2$	non-hyperbolic
		$a_2 = 2$	non-hyperbolic
	$c_1 < c < \tilde{c}$	$0 < a_2 < 2$	sink
		$a_2 > 2$	saddle
		$a_2 = 2$	non-hyperbolic

2.3. Global attractivity of positive equilibrium point

In this section, we consider the global asymptotic stability of the equilibrium point with the help of Lemmas 3–5 from [30] and Lemmas 2.1 and 2.2 from [40].

Theorem 2.5. *Suppose that* $0 < a_2 < 2$, $0 < k^{**} < k < k^*$ *holds and* $E^*(x^*, a_2)$ *is globally attractive, i.e.,*

$$\lim_{n\to\infty} x(n) = x^*, \lim_{n\to\infty} y(n) = a_2, \tag{2.3}$$

where $k^* = \frac{e_1-e_2-ca_2}{(e_2+ca_2)a_2}$ *and* $k^{**} = \frac{e_1-\ln 2-1-e_2-ca_2}{(\ln 2+1+e_2+ca_2)a_2}$.

Proof. According to Lemma 4 in [30], if $0 < a_2 < 2$ holds, then

$$\lim_{n\to\infty} y(n) = a_2.$$

For sufficiently small ε, there exists an integer N_1, such that for all $n > N_1$,

$$y(n) > a_2 - \varepsilon. \tag{2.4}$$

From Lemma 2.1 and 2.2 in [40], we obtain:

$$\liminf_{n\to+\infty} y(n) \geq \min\left\{a_2 \exp\left(a_2 - \exp(a_2 - 1)\right), a_2\right\} := H_1. \tag{2.5}$$

Now, we consider the following system:

$$x_1(n+1) = x_1(n)\exp\left(\frac{e_1}{1+ka_2} - e_2 - x_1(n) - ca_2\right). \tag{2.6}$$

Apparently, $x_1^* = x^*$ is the positive equilibrium point of the system. Suppose $\{x_1(n)\}$ is any positive solution of system (1.5). From Lemma 3 in [30], if $0 < e_1 - (1+ka_2)(e_2+ca_2) < 2$, we know that $\lim\limits_{n\to\infty} x_1(n) = x^*$. Thus, we only need to prove that

$$\lim_{n\to\infty}(x(n) - x_1(n)) = 0.$$

Assume that

$$x(n) = x_1(n)\exp[k_1(n)].$$

Therefore, our main goal is to prove $\lim\limits_{n\to\infty} k_1(n) = 0$.

The first equation of (1.5) is equivalent to

$$\begin{aligned} k_1(n+1) &= \ln x(n) + \tfrac{e_1}{1+ky(n)} - e_2 - x(n) - cy(n) - \ln x_1(n+1) \\ &= k_1(n)\Big(1 - x_1(n)\exp[\theta_1(n)k_1(n)]\Big) - \Big(c + \tfrac{ke_1}{(1+a_2k)(1+ky(n))}\Big)\Big(y(n) - a_2\Big). \end{aligned} \tag{2.7}$$

Then, $x_1(n)\exp[\theta_1(n)k_1(n)]$ is between $x_1(n)$ and $x(n)$, and here $\theta_1(n) \in [0,1]$.

It follows from (2.5) that

$$\frac{ke_1}{(1+a_2k)(1+ky(n))} \le \frac{ke_1}{(1+a_2k)(1+kH_1)} := W_1.$$

Obviously,

$$\begin{aligned} &x(n)\exp\big[\frac{e_1}{1+(a_2+\varepsilon)k} - e_2 - c(a_2+\varepsilon) - x_1(n)\big] \\ &\le x(n+1) \le x(n)\exp\big[\frac{e_1}{1+a_2k} - e_2 - ca_2 - x_1(n)\big], \end{aligned}$$

holds. Thus, according to Lemma 2.1 and 2.2 in [40], it immediately follows that:

$$\begin{aligned} \limsup_{n\to+\infty} x(n) &\le \exp\big(\frac{e_1}{1+a_2k} - e_2 - ca_2 - 1\big) := Q_1, \\ \liminf_{n\to+\infty} x(n) &\ge \min\Big\{\Big(\frac{e_1}{1+(a_2+\varepsilon)k} - e_2 - c(a_2+\varepsilon)\Big)\exp\big[-e_2 \\ &\quad + \frac{e_1}{1+(a_2+\varepsilon)k} - c(a_2+\varepsilon) - Q_1\big], \frac{e_1}{1+(a_2+\varepsilon)k} \\ &\quad - e_2 - c(a_2+\varepsilon)\Big\} := M_1. \end{aligned}$$

Setting $\varepsilon \to 0$ in the above inequalities leads to

$$\limsup_{n\to+\infty} x_1(n) \le \exp\big(\frac{e_1}{1+a_2k} - e_2 - ca_2 - 1\big) = Q_1,$$

$$\liminf_{n\to+\infty} x_1(n) \geq \min\left\{\left(\frac{e_1}{1+a_2k} - e_2 - ca_2\right)\exp\left[\frac{e_1}{1+a_2k}\right.\right.$$
$$\left.\left. - e_2 - ca_2 - Q_1\right], \frac{e_1}{1+a_2k} - e_2 - ca_2\right\} \geq M_1.$$

Hence, taking an integer $N_2 > N_1$, for $\xi > 0$ small enough, when $n \geq N_2$, the following inequality holds:

$$M_1 - \xi \leq x(n),\ x_1(n) \leq Q_1 + \xi,\ n \geq N_2. \tag{2.8}$$

Assume

$$\lambda_1 = \max\{|1 - M_1|, |1 - Q_1|\}.$$

Now, let

$$\lambda_{\varepsilon 1} = \max\{|1 - (M_1 - \xi)|, |1 - (Q_1 + \xi)|\}. \tag{2.9}$$

Therefore,

$$|k_1(n+1)| \leq \max\{|1 - (M_1 - \xi)|, |1 - (Q_1 + \xi)|\}|k_1(n)| + (c + W_1)\varepsilon$$
$$= \lambda_{\varepsilon 1} + (c + W_1)\varepsilon,\ n \geq N_2.$$

The following equation can be obtained:

$$|k_1(n)| \leq \lambda_{\varepsilon 1}^{n-N_2}|k_1(N_2)| + \frac{1 - \lambda_{\varepsilon 1}^{n-N_2}}{1 - \lambda_{\varepsilon 1}}(c + W_1)\varepsilon,\ n \geq N_2. \tag{2.10}$$

Considering $\lambda_{\varepsilon 1} < 1$, then $\lim_{n\to+\infty} k_1(n) = 0$, i.e., $\lim_{n\to+\infty}[x(n) - x_1(n)] = 0$ is established if $\lambda_1 < 1$. Since

$$1 - Q_1 < 1 - M_1 < 1,$$

$\lambda_1 < 1$ is equivalent to $1 - Q_1 > -1$, i.e.,

$$\frac{e_1}{1+a_2k} - e_2 - ca_2 < 1 + \ln 2.$$

Hence, Theorem 3.1 is proved.

2.4. Global attractivity of boundary equilibrium

Now, we discuss the global attractivity of E_1 with the help of Lemma 6 and 7 from [30].

Theorem 2.6. *Assuming that $k > k^*$, $0 < a_2 < 2$ holds, and $E_1(0, a_2)$ is globally attractive, i.e.,*

$$\lim_{n\to\infty} x(n) = 0, \lim_{n\to\infty} y(n) = a_2.$$

Proof. The proof of $\lim_{n\to\infty} y(n) = a_2$ follows the same process as the one in Theorem 2.5 above, so it is omitted here. Next, we prove that $\lim_{n\to\infty} x(n) = 0$.

Consider the auxiliary equation:

$$x_2(n+1) = x_2(n)\exp\left(\frac{e_1}{1+ka_2} - e_2 - x_2(n) - cy(n)\right),$$

combined with the second equation of system (1.5), for all $i \in \mathbb{N}$, we have

$$\begin{aligned} \ln \frac{x_2(i+1)}{x_2(i)} &= \frac{e_1}{1+ka_2} - e_2 - x_2(i) - cy(i) \\ \ln \frac{y(i+1)}{y(i)} &= a_2 - y(i). \end{aligned} \tag{2.11}$$

According to the Theorem 2.6, we have $\frac{\frac{e_1}{1+ka_2}-e_2}{a_2} < c$, i.e.,

$$\frac{e_1}{1+ka_2} - e_2 - ca_2 < 0. \tag{2.12}$$

Therefore, the following inequality holds:

$$\frac{\frac{e_1}{1+ka_2} - e_2}{a_2} < \frac{s}{h} < c,$$

where s and h are positive numbers. Then,

$$hc - s > 0 \tag{2.13}$$

and there exist $\delta > 0$ such that

$$h(\frac{e_1}{1+ka_2} - e_2) - sa_2 < -\delta < 0. \tag{2.14}$$

From (2.11)–(2.14), we have

$$\begin{aligned} h \ln \frac{x_2(i+1)}{x_2(i)} - s \ln \frac{y(i+1)}{y(i)} &\le [h(\frac{e_1}{1+ka_2} - e_2) - sa_2] \\ &\quad - \Big[hx_2(i) + (hc-s)y(i)\Big] \\ &\le h(\frac{e_1}{1+ka_2} - e_2) - sa_2 < -\delta < 0. \end{aligned}$$

Summing up the above formulas, we can get:

$$\begin{aligned} &\sum_{i=1}^{n} \left(h \ln \frac{x_2(i+1)}{x_2(i)} - s \ln \frac{y(i+1)}{y(i)} \right) \\ &= h \ln \frac{x_2(n)}{x_2(0)} - s \ln \frac{y(n)}{y(0)} < -\delta n. \end{aligned}$$

Then,

$$x_2(n) < x_2(0) \left(\frac{y(n)}{y(0)} \right)^{\frac{s}{h}} \exp\left(-\frac{\delta}{h} n \right). \tag{2.15}$$

According to Lemma 2.1 in [40] and $y(n+1) \le y(n)\exp(a_2 - y(n))$, it holds that:

$$\limsup_{n \to +\infty} y(n) \le \exp(a_2 - 1).$$

Therefore, taking an integer $N_2 > N_1$, for $\varepsilon > 0$, when $n \geq N_2$, $y(n) \leq \exp(a_2 - 1) + \varepsilon := M$ is established. So, the inequality (2.15) is equivalent to

$$x_2(n) < x_2(0)\Big(\frac{M}{y(0)}\Big)^{\frac{s}{h}} \exp\Big(-\frac{\delta}{h}n\Big), \forall n \geq N_2.$$

Thus,

$$\lim_{n\to\infty} x_2(n) = 0. \tag{2.16}$$

Therefore, if we want to prove $\lim_{n\to\infty} x(n) = 0$, we only need to prove

$$\lim_{n\to\infty} (x(n) - x_2(n)) = 0,$$

Assume that

$$x(n) = x_2(n) \exp[k_2(n)].$$

Therefore, we can convert what we need to prove into the proof $\lim\limits_{n\to\infty} k_2(n) = 0$.

By a similar process of proof as in Theorem 2.5, we have that when

$$\frac{e_1}{1 + ka_2} - e_2 - ca_2 < \ln 2 + 1, \tag{2.17}$$

$\lim\limits_{n\to\infty} k_2(n) = 0$ holds. Combining condition (2.11) and condition (2.16), we have that $\lim_{n\to\infty} x(n) = 0$ holds when $e_1/(1 + ka_2) - e_2 - ca_2 < 0$. Hence, Theorem 2.6 is proved.

3. Bifurcation analysis

Based on the above proofs, it becomes evident that the system (1.5) exhibits several bifurcation types at its fixed points. In the subsequent discussion, we will examine these potential bifurcations by employing the center manifold [41] and bifurcation theory [42, 43].

3.1. Flip bifurcation at $E_1(0, a_2)$, $E_2(e_1 - e_2, 0)$

Theorem 2.2 states that if $a_2 = 2$ and $e_1 \neq (1 + a_2k)(ca_2 + e_2)$ holds, then one of the eigenvalues of $E_1(0, a_2)$ is -1 and another one is neither 1 nor –1. These requirements suggest that all parameters belong to the set T_A:

$$T_A := \{(e_1, e_2, k, c, a_2) : a_2 = 2, e_1 \neq (1 + a_2k)(ca_2 + e_2), e_1, e_2, c > 0, k \geq 0\}.$$

At this point, the central manifold of system (1.5) at $E_1(0, a_2)$ is $x = 0$. Therefore, the restricted system of (1.5) to it is:

$$y_{n+1} = f(y_n) = y_n \exp(a_2 - y_n).$$

$f'(a_2) = -1$ is obvious, so it can be seen that a flip bifurcation occurs at $E_1(0, a_2)$. Figure 3(a) depicts the bifurcation diagram about E_1.

Based on conclusion (4) of Theorem 2.3, we obtain that all parameters belong to the set T_B:

$$T_B := \{(e_1, e_2, k, c, a_2) : e_1 = e_2 + 2, a_2, e_2, c > 0, k \geq 0\}.$$

We can easily know that the central manifold of system (1.5) at $E_2(e_1 - e_2, 0)$ is $y = 0$. So the restricted system of (1.5) to it is:

$$x_{n+1} = g(x_n) = x_n \exp(e_1 - e_2 - x_n).$$

Thus, we have $g'(e_1 - e_2) = -1$. Figure 3(b) depicts the bifurcation diagram about E_2. Moreover, as illustrated in Figure 3, the maximum Lyapunov exponents (MLE) for(a),(b) are depicted in (c) and (d), respectively.

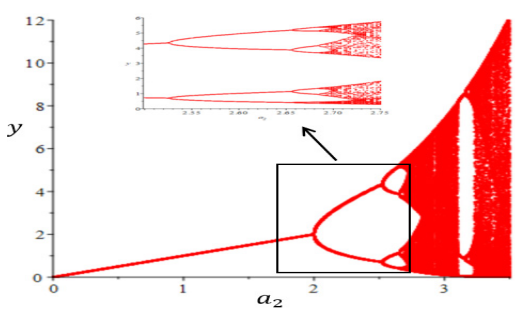

(a) The bifurcation diagram

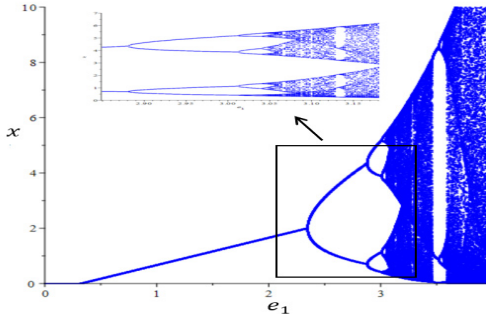

(b) The bifurcation diagram

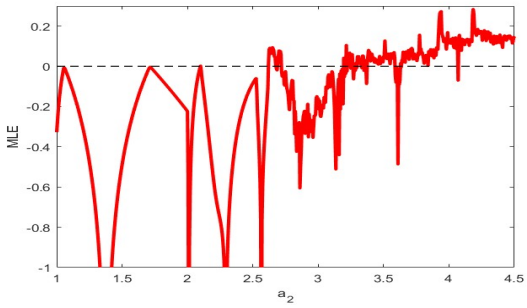

(c) The MLE

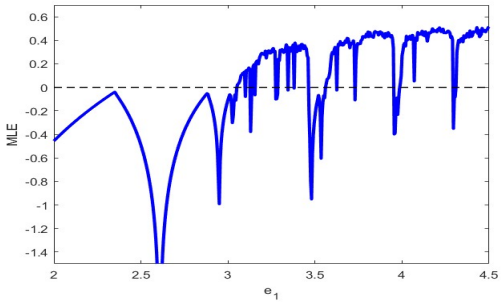

(d) The MLE

Figure 3. (a) represent flip bifurcation diagrams of $E_1(0, a_2)$ with $e_1 = 4, k = 0.3, e_2 = 0.3, c = 0.2$; (b) represent flip bifurcation diagrams of $E_2(e_1 - e_2, 0)$ with $k = 0.12, e_2 = 0.3, c = 0.2, a_2 = 0.1$.

3.2. Flip bifurcation at $E^*(x^*, a_2)$

According to Theorem 2.4, if $e_1^* = (1 + ka_2)(2 + e_2 + a_2c)$, then at $E^*(x^*, a_2)$, one eigenvalue is -1 and another one is neither 1 nor -1, These conditions imply that all parameters belong to the set F_c:

$$F_c := \left\{(e_1^*, e_2,\ k,\ c,\ a_2) : e_1^* = (1 + ka_2)(2 + e_2 + a_2c),\ a_2 \neq 2,\ e_2,\ c,\ a_2 > 0, k \geq 0\right\}.$$

If the condition of $(e_1^*, e_2,\ k,\ c,\ a_2) \in F_c$ is satisfied, flip bifurcation may occur. Thus, suppose δ is a bifurcation parameter satisfying $\|\delta\| \ll 1$. Then, system (1.5) can be expressed as follows:

$$\begin{pmatrix} x \\ y \end{pmatrix} \to \begin{pmatrix} x \exp\left(\dfrac{e_1^* + \delta}{1 + ky} - e_2 - x - cy\right) \\ y \exp(a_2 - y) \end{pmatrix}. \tag{3.1}$$

First, we transform E^* to the origin by using the transformation $u = x - x^*$, $v = y - a_2$ and then utilize Taylor expansion, turning the mapping (3.1) into

$$\begin{pmatrix} u \\ v \end{pmatrix} \to \begin{pmatrix} -1 & a_{010} \\ 0 & 1 - a_2 \end{pmatrix} \begin{pmatrix} u \\ v \end{pmatrix} + \begin{pmatrix} f_3(u, v, \delta) \\ g_3(u, v, \delta) \end{pmatrix}, \tag{3.2}$$

where

$$\begin{aligned} f_3(u, v, \delta) &= z_{101}uv + s_{110}u\delta + z_{011}v^2 + s_{220}v\delta + z_{022}u^2\delta + s_{330}u^3 + z_{033}uv^2 \\ &\quad + s_{440}uv\delta + s_{550}v^3 + z_{055}v^2\delta + s_{660}v\delta^2 + O((|u| + |v| + |\delta|)^4), \\ g_3(u, v, \delta) &= \frac{(a_2 - 2)v^2}{2} - \frac{(a_3 - 3)v^3}{6} + O((|u| + |v| + |\delta|)^4) \end{aligned}$$

and

$$\begin{aligned} &a_{010} = -2z_{101},\ z_{101} = \frac{2a_2ck + e_2k + c + 2k}{a_2k + 1},\ s_{110} = -\frac{1}{a_2k + 1}, \\ &z_{011} = z_{101}^2 + \frac{2k^2(a_2c + e_2 + 2)}{a_2k + 1},\ s_{220} = -\frac{z_{011}}{a_2k + 1} - \frac{2k}{(a_2k + 1)^2}, \\ &s_{330} = \frac{1}{6},\ z_{022} = \frac{1}{2(a_2k + 1)},\ z_{033} = \frac{z_{011}}{2},\ s_{440} = \frac{z_{011}}{a_2k + 1} + \frac{k}{(a_2k + 1)^2}, \\ &s_{550} = -\frac{z_{011}z_{101}}{3} - \frac{z_{101}^2(4a_2ck^2 + 6e_2k^2 + 11k^2}{3(1 + a_2k)} - \frac{k^2(-2e_2k - 2e_2c + 11e_2k - 3c + 6k)}{3(1 + a_2k)^3}, \\ &z_{055} = \frac{z_{011}}{2(a_2k + 1)} + \frac{2ck}{(1 + a_2k)^2} - \frac{2k(a_2c + e_2 + 3)}{(1 + a_2k)^3},\ s_{660} = -\frac{k}{(a_2k + 1)^2}. \end{aligned}$$

Next, we use the invertible transformation:

$$\begin{pmatrix} u \\ v \end{pmatrix} = \begin{pmatrix} a_{010} & a_{010} \\ 0 & 2 - a_2 \end{pmatrix} \begin{pmatrix} X \\ Y \end{pmatrix}.$$

Equation (3.2) can be rewritten as

$$\begin{pmatrix} X \\ Y \end{pmatrix} \to \begin{pmatrix} -1 & 0 \\ 0 & 1 - a_2 \end{pmatrix} \begin{pmatrix} X \\ Y \end{pmatrix} + \begin{pmatrix} f_4(u, v, \delta) \\ g_4(u, v, \delta) \end{pmatrix}, \tag{3.3}$$

where

$$\begin{aligned} u &= a_{010}(X + Y), v = (2 - a_2)Y, \\ f_4(u, v, \delta) &= b_{101}uv + a_{110}u\delta + b_{011}v^2 + a_{220}v\delta + a_{330}u^3 + b_{033}uv^2 + a_{440}uv\delta \\ &\quad + a_{550}v^3 + b_{550}v^2\delta + a_{660}v\delta^2 + b_{066}u^2\delta + O((|u| + |v| + |\delta|)^4), \end{aligned}$$

$$g_4(u,v,\delta) = -\frac{1}{2}v^2 - \frac{a_3-3}{6(a_2-2)}v^3 + O((|u|+|v|+|\delta|)^4)$$

and

$$b_{110} = \frac{z_{101}}{a_{010}},\ a_{110} = \frac{s_{110}}{a_{010}},\ b_{011} = \frac{z_{011}}{a_{010}} + \frac{1}{2},\ a_{220} = \frac{s_{220}}{a_{010}},$$
$$a_{330} = \frac{s_{330}}{a_{010}},\ b_{033} = \frac{z_{033}}{a_{010}},\ a_{440} = \frac{s_{440}}{a_{010}},\ a_{550} = \frac{s_{550}}{a_{010}} - \frac{a_2-3}{6(a_2-2)},$$
$$b_{550} = \frac{z_{055}}{a_{010}},\ a_{660} = \frac{s_{660}}{a_{010}},\ b_{066} = \frac{z_{022}}{a_{010}}$$

According to the central manifold theorem, there exists a central limit $W_1^c(0,0,0)$, which can be expressed as

$$W_1^c(0,0,0) = \Big\{(X,Y,\delta) : Y = h(X,\delta), h(0,0) = 0, Dh(0,0) = 0\Big\},$$

where

$$h(X,\delta) = t_1X^2 + t_2X\delta + t_3\delta^2 + O((|X|+|\delta|)^3. \tag{3.4}$$

Based on (3.3), $Y = h(X,\delta)$ must satisfy:

$$h(-X + f_4(X,h(X,\delta),\delta),\delta) = (1-a_2)h(X,\delta) + g_4(X,h(X,\delta),\delta).$$

By calculation, we obtain $t_1 = t_2 = t_3 = 0$. Thus, the map (3.3) can be written as :

$$G^* : X \to -X + c_{110}\delta + c_{011}X\delta + c_{220}\delta^2 + c_{330}X^3 + c_{033}X\delta^2 + c_{440}\delta^3 + O((|X|+|\delta|)^3),$$

where

$$c_{110} = \frac{2}{a_{010}(ka_2+1)}\delta,\ c_{011} = -\frac{1}{ka_2+1},\ c_{220} = \frac{1}{(ka_2+1)^2a_{010}},$$
$$c_{330} = \frac{a_{010}^2}{6},\ c_{033} = -\frac{1}{2(ka_2+1)^2},\ c_{440} = \frac{1}{3(ka_2+1)^3}.$$

Then, we have:

$$\varpi_1 = (G^*_{X\delta} + \frac{1}{2}G^*_\delta G^*_{XX})|_{(X,\delta)=(0,0)} = -\frac{1}{ka_2+1} \neq 0,$$
$$\varpi_2 = (\frac{1}{6}G^*_{XXX} + (\frac{1}{2}G^*_{XX})^2)|_{(X,\delta)=(0,0)} = \frac{a_{010}^2}{6} \neq 0.$$

Consequently, the following conclusions can be drawn.

Theorem 3.1. *If* $(e_1^*, e_2,\ k,\ c,\ a_2) \in F_c$, *then the system* (1.5) *undergoes flip bifurcation at* $E^*(x^*, a_2)$. *(see Figure 7)*

3.3. Transcritical bifurcation at $E_0(0,0)$

According to Theorem 2.1, if $e_1 = e_2$, then at $E_0(0,0)$, one eigenvalue is 1 and another one is neither 1 nor -1. These conditions mean that all of the parameters are in the set F_d:

$$F_d := \Big\{(e_1,\ e_2,\ k,\ c,\ a_2)\colon e_1 = e_2,\ e_1, e_2,\ c,\ a_2 > 0, k \geq 0\Big\}.$$

Taking e_1 as the bifurcation parameter and setting η as the disturbance parameter, the map is as follows:

$$\begin{pmatrix} x \\ y \end{pmatrix} \to \begin{pmatrix} x\exp\big(\dfrac{e_1^* + \eta}{1+ky} - e_2 - x - cy\big) \\ y\exp(a_2 - y) \end{pmatrix}. \tag{3.5}$$

Next, a Taylor expansion is performed at the origin. Then, (3.5) becomes

$$\begin{pmatrix} x \\ y \end{pmatrix} \to \begin{pmatrix} 1 & 0 \\ 0 & \lambda_2 \end{pmatrix}\begin{pmatrix} x \\ y \end{pmatrix} + \begin{pmatrix} f(x,y,\eta) \\ g(x,y,\eta) \end{pmatrix}, \tag{3.6}$$

where

$$\begin{aligned} f(x,y,\eta) &= -x^2 + x\eta - (e_2k + c)yx + \frac{x^3}{2} - x^2\eta + (e_2k + e_1)yx^2 + \frac{x\eta^2}{2} \\ &\quad \frac{(e_2^2k^2 + 2ce_2k + 2e_2k^2 + c^2)y^2x}{2} - (e_2k + c + k)yx\eta + O((|x| + |y| + |\eta|)^4), \\ g(x,y,\eta) &= -\lambda_2 y^2 + \frac{\lambda_2}{2}y^3 + O((|x| + |y| + |\eta|)^4), \end{aligned}$$

Setting the approximate central mainfold $W_2^c(0,0,0)$ of (3.6) as

$$W_2^c(0,0,0) = \Big\{(x,y,\eta)\colon y = h_1x^2 + h_2x\eta + h_3\eta^2 + O((|x| + |\eta|)^3)\Big\},$$

for x and η sufficiently small. By a simple coefficient comparison, we can obtain $h_1 = h_2 = h_3 = 0$. Therefore, the map on the center manifold is:

$$K : x \to x - x^2 + x\eta + \frac{1}{2}x^3 - x^2\eta + \frac{1}{2}\eta^2x + O((|x| + |\eta|)^4).$$

By simple compulation, we have:

$$\begin{cases} \mathcal{L}_1 \triangleq \left(\dfrac{\partial^2 K}{\partial x^2}\right)_{(0,0)} = -2 \neq 0, \\ \mathcal{L}_2 \triangleq \left(\dfrac{\partial^2 K}{\partial x \partial \eta}\right)_{(0,0)} = 1 \neq 0. \end{cases}$$

Hence, we draw the following conclusion about transcritical bifurcation.

Theorem 3.2. *If $(e_1, e_2,\ k,\ c,\ a_2) \in F_d$, then system (1.5) experiences transcritical bifurcation at $E_0(0,0)$.*

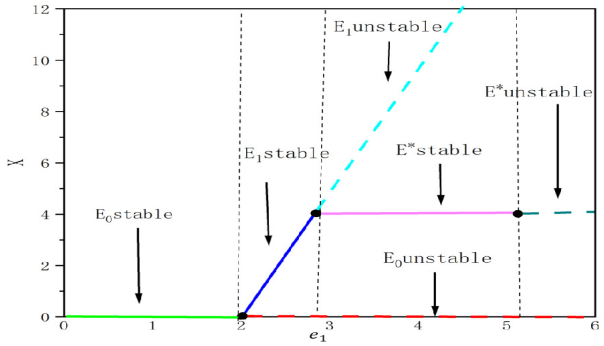

Figure 4. Transcritical bifurcation diagram in $e_1 - x$ plane with $e_2 = 2, a_2 = 1, c = 0.2, k = 0.3$.

3.4. Chaos control

Considering that the flip bifurcation may lead to chaos, in this section, we focus on controlling the generation of chaos. Combined with the method of hybrid control, the related control system (1.5) is expressed as follows:

$$\begin{cases} x_{n+1} = \rho x_n \exp\left(\dfrac{e_1}{1+ky} - e_2 - x - cy_n\right) + (1-\rho)x_n, \\ y_{n+1} = \rho y_n \exp\left(a_2 - y_n\right) + (1-\rho)y_n, \end{cases} \tag{3.7}$$

where $\rho \in (0, 1)$. The Jacobian matrix of $E^*(x^*, a_2)$ in the control system (3.7) is as follows:

$$J(E^*) = \begin{pmatrix} 1 - \dfrac{\rho(e_1 - (1+a_2k)(ca_2+e_2))}{1+ka_2} & -\rho x^*\left(\dfrac{e_1 k}{(1+ka_2)^2}\right) \\ 0 & 1-\rho a_2 \end{pmatrix}. \tag{3.8}$$

Its eigenvalues are $\lambda_1 = 1 - \rho\Big(e_1 - (1+a_2k)(ca_2+e_2)\Big)/(1+ka_2) < 1$ and $\lambda_2 = 1 - \rho a_2 < 1$, respectively. Hence, we have the following outcome:

Theorem 3.3. *The controlled system* (1.5) *is locally asymptotically stable at* $E^*(x^*, a_2)$ *when*

$$0 < \rho < \min\left\{\frac{2}{a_2}, \frac{2(1+ka_2)}{e_1 - (1+a_2k)(ca_2+e_2)}, 1\right\}.$$

4. Numerical examples and discussions

In this section, we will illustrate the accuracy of relevant conclusions and explore the influence of the fear effect on the system through numerical simulations.

Example 1. *(the effect of fear effect on* E_1*)*

1) Given the values $(e_1, a_2, e_2, c, k) = (1, 1.7, 0.4, 0.3, 0.1)$*, it can be observed that* $(a_2k+1)(a_2c+e_2) = 1.06$*, which is larger than* e_1*. Additionally, it is known that* $0 < a_2 < 2$*. Consider the three sets of initial values:* $(0.3, 0.8)$*,* $(0.6, 0.2)$ *and* $(1.2, 0.7)$*. As depicted in Figure 5(a), it can be observed that* E_1

exhibits local asymptotic stability. The correctness of the result of Theorem 3 is affirmed. Furthermore, to investigate the impact of the fear effect on the local stability of E_1, we varied the parameter k from 0.1 *to* 5. *The findings are depicted in Figure 5(b). It can be observed that the presence of fear induces an increase in the local stability of E_1, thereby expediting the process of extinction for the first species.*

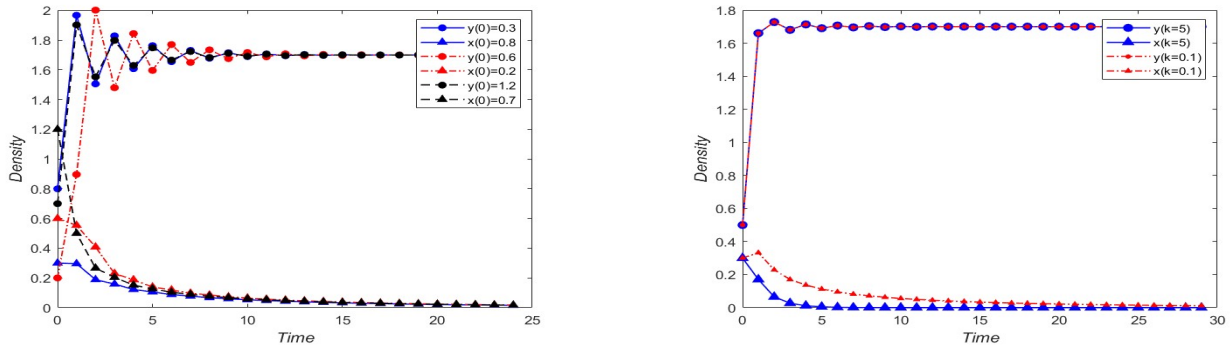

(a) (b)

Figure 5. (a) Local stability of E_1 with $e_1 = 1, a_2 = 1.7, e_2 = 0.4, c = 0.3, k = 0.1$. (b) The fear effect on E_1 with $k = 0.1, k = 5$.

2) Given the values $(e_1, e_2, c, k) = (4, 0.5, 1, 2)$ *and the condition* $a_2 > 2$, *we observe that* $e_1 = 4 < (a_2k + 1)(a_2c + e_2)$. *satisfying condition (3) of Theorem 2.2 and indicating that E_1 is unstable at this particular moment. Next, we select a_2 as the bifurcation parameter to investigate the impact of a_2 on the system. As depicted in Figure 6, when the value of a_2 grows, the first species will undergo extinction, whereas the second species will experience a state of chaos. Furthermore, the aforementioned conditions fail to meet the requirements stated in Theorem 2.6, namely the conditions for achieving global stability of E_1. Therefore, this example also provides additional evidence about the plausibility of the conditions outlined in Theorem 2.6.*

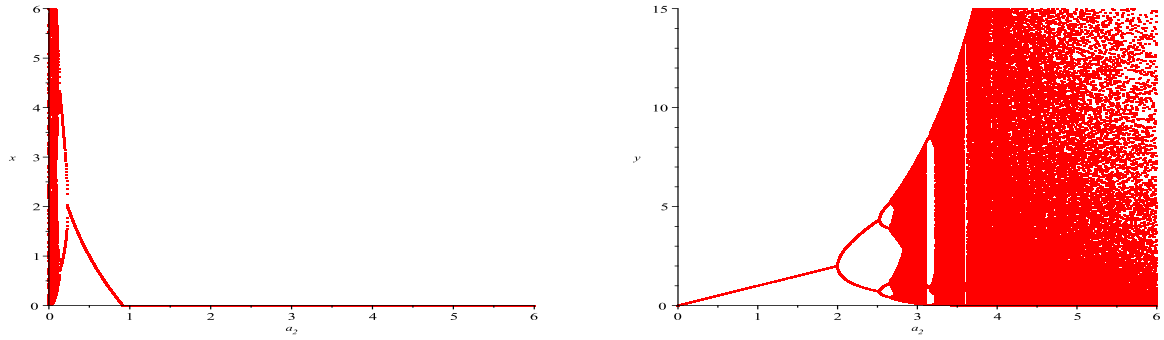

(a) (b)

Figure 6. (a) The population density of x with bifurcating parameter a_2 and (b) the population density of y with bifurcating parameter a_2.

Example 2. *(the fear effects on the first species)*

Case 1: Assuming that the second species is global stability, i.e., $0 < a_2 < 2$

When the value of k is set to 0.3*, Figure 7(a) illustrates periodic-2, 4 and 8 orbits. To provide a more intuitive observation of periodic orbits and chaotic sets, we present the phase diagrams corresponding to each stage of Figure 7(a) for six different values of* e_1*:* $2, 3.25, 3.6, 4.1, 4.2, 4.3$*. (as shown in Figure 8). The first species exhibits stability when* e_1 *falls between* 0 *and* 3.25*, becoming unstable when* e_1 *exceeds* 3.25*. It is observed that with an increase in the birth rate, the initial species exhibits instability or even chaotic behavior. In this study, our goal is to investigate the impact of the fear effect on the first species under conditions of chaos. We set the parameter* e_1 *to a value of 4.3 and utilize the bifurcation parameter k. The stability of* $E^*(x^*, a_2)$ *is observed to be dependent on the value of k. Specifically,* $E^*(x^*, a_2)$ *is unstable for* $0 < k < 0.65$ *and stable for* $k > 0.65$*. The analysis of Figure 7(b) reveals that the fear effect significantly contributes to preserving stability in the first species, especially when the second species achieves global stability.*

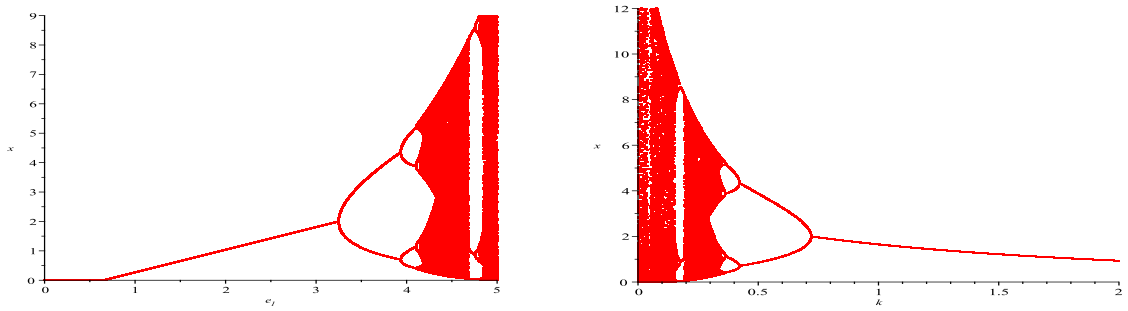

(a) e_1 is the bifurcation parameter (b) k is the bifurcation parameter

Figure 7. System (1.5) has a flip bifurcation diagram at point $E^*(2.57, 1)$ with $a_2 = 1, c = 0.2, e_2 = 0.3$.

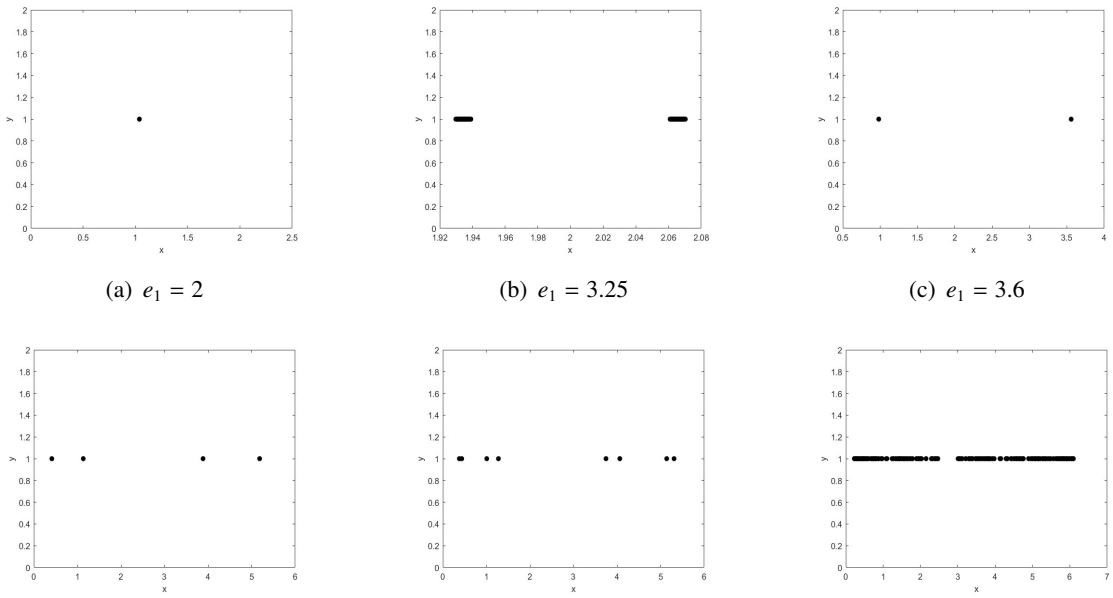

(a) $e_1 = 2$ (b) $e_1 = 3.25$ (c) $e_1 = 3.6$

(d) $e_1 = 4.1$ (e) $e_1 = 4.12$ (f) $e_1 = 4.3$

Figure 8. Phase portraits for various values of e_1 corresponding to Figure 7(a).

Case 2: Assuming that the second species is chaos, i.e., $a_2 > 2$.

When $a_2 > 2$, *the second species exhibits chaotic behavior, leading to the following scenarios. In this chaotic state, it is observed that the fear effect no longer has the effect of stabilizing the first species. Moreover, with the increase of the parameter k, the density of the first species decreases, eventually leading to its extinction when* $k > k^*$.

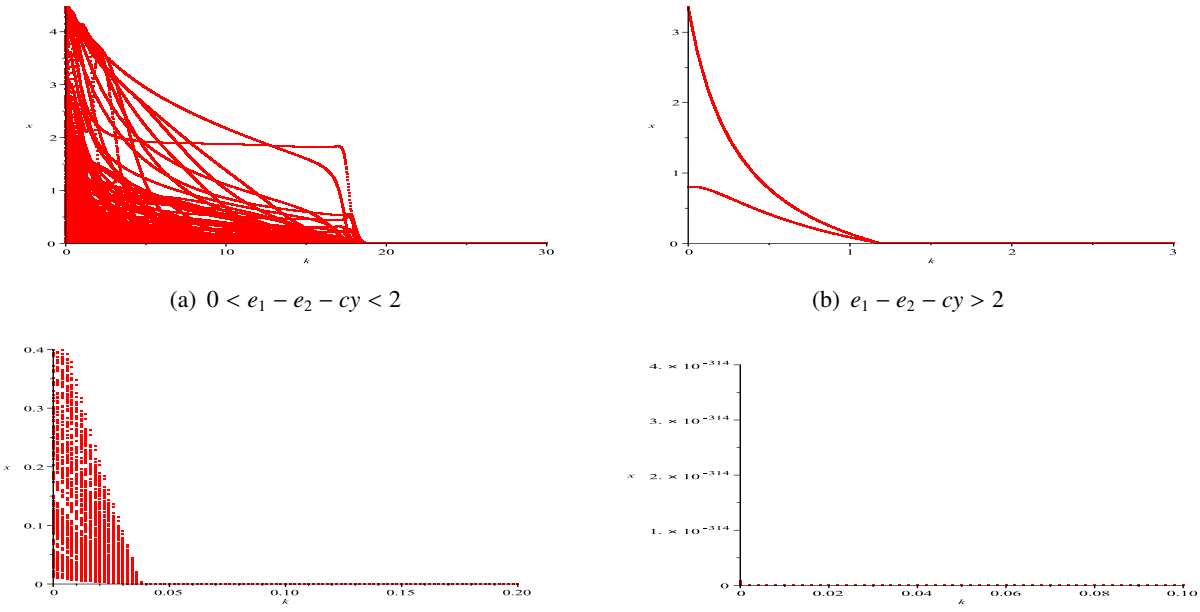

(a) $0 < e_1 - e_2 - cy < 2$ (b) $e_1 - e_2 - cy > 2$

(c) $0 < e_1 - e_2 < 2$ (d) $e_1 - e_2 < 0$

Figure 9. The bifurcation plot of x corresponding to the bifurcating parameter k. (a) $(a_2, c, e_1, e_2) = (4, 0.2, 3, 0.5)$; (b) $(a_2, c, e_1, e_2) = (2.1, 0.2, 3, 0.5)$; (c) $(a_2, c, e_1, e_2) = (4, 0.2, 2, 1)$; (d) $(a_2, c, e_1, e_2) = (4, 0.2, 1, 1.1)$.

Figure 10 depicts the effect of the parameters e_1 *and k, as well as the parameters* a_2 *and k, on the bifurcation.*

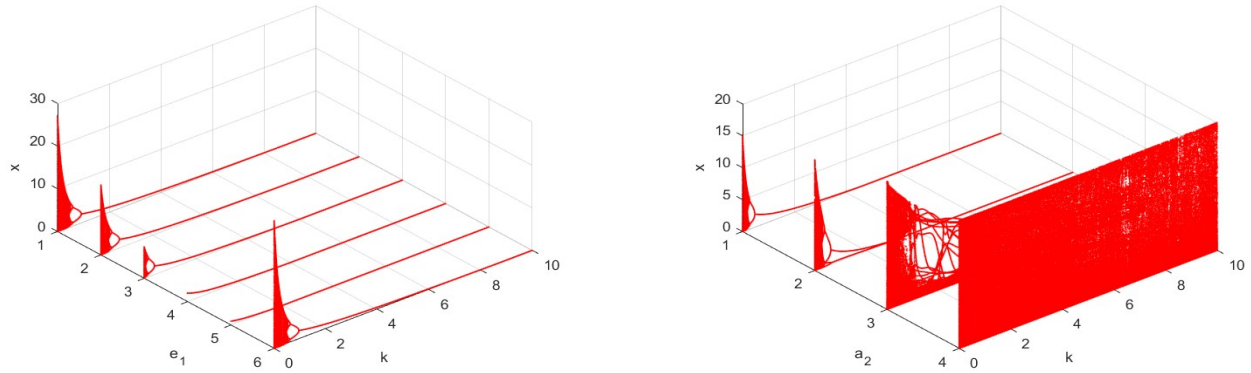

(a) (b)

Figure 10. Bifurcation diagrams of system (1.5) in (a) $(k, e_1, x) - space$, (b) $(k, a_2, x) - space$.

Furthermore, when the parameter k is set to zero, a comparison between system (1.1) *and system* (1.5) *reveals that the variable a_1 in system* (1.1) *corresponds to the difference between e_1 and e_2 in system* (1.5)*. Additionally, both b_1 and c_2 in system* (1.1) *assume a value of* 1 *in system* (1.5)*. Consequently, when the parameter values of system* (1.5) *are set to $(a_2, c, e_2, e_1) = (3, 0.2, 0.3, 2.3)$, it corresponds to the parameter values of system* (1.1) *being $(a_2, c_1, a_1, c_2, b_1) = (3, 0.2, 2, 1, 1)$. At this time, it is observed that $a_1/c_1 > a_2/c_2$. According to the findings of Theorem A, it can be deduced that the positive equilibrium point in system* (1.1) *is globally stable. However, the positive equilibrium point in system* (1.5) *is unstable, and there exists a potential for flip bifurcation. Consequently, the discrete model exhibits more intricate dynamical behavior in comparison to the continuous model.*

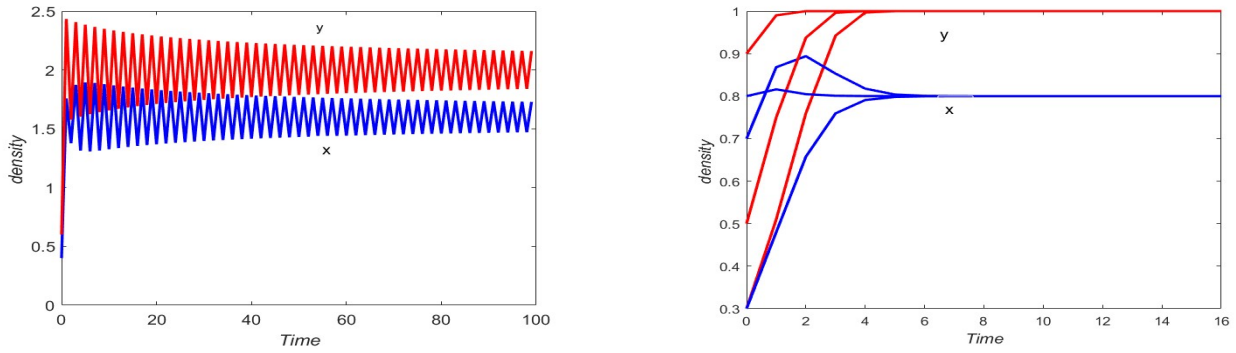

(a) (b)

Figure 11. (a) Stability of positive equilibrium points of system (1.5) and (b) stability of positive equilibrium points of system (1.1) with the initial value is set to $(0.4, 0.6)$, $(0.3, 0.7)$, $(0.8, 0.9)$.

Example 3. *(the effect of fear effect on E^*)*

We examine the stability of the positive equilibrium point $E^*(x^*, a_2)$. The parameters are assigned values of $(a_2, e_2, c, e_1) = (0.5, 1, 0.2, 3)$, and the initial values (x_0, y_0) are set to $(0.4, 0.3)$, $(0.5, 0.8)$ *and* $(1.1, 0.6)$ *accordingly. Based on the conditions stated in Theorem 2.5, it can be concluded that when $k \in (0.07, 3.4545)$, the positive equilibrium point $E^*(x^*, a_2)$ is globally stable. To verify the feasibility of Theorem 2.5, we select $k = 2$, as depicted in Figure 12(a). It can be observed that at this value of k, the equilibrium point E^* remains globally stable. Furthermore, in order to investigate the effect of the fear effect on the global stability of E^*, we chose $k = 4$. The results show that the fear effect affects the global stability of the positive equilibrium point and reduces the density of the first species. This reduction in density eventually leads to the extinction of the first species.*

The values assigned to (a_2, e_2, c, e_1) are $(1, 0.5, 0.3, 4)$*. For this set of parameters, the values of k^{**} and k^* are* 0.60 *and* 4*, respectively. We will use k as the bifurcation parameter to investigate the influence of k on the stability of E^*. At this time, the second species is stable. Combined with Figure 13(a), we can see that when $k^{**} < k < k^*$, E^* is stable; when $k > k^*$, the first species becomes extinct. Therefore, we can conclude that an appropriate value of k promotes the convergence of the first species from a chaotic state to stability.*

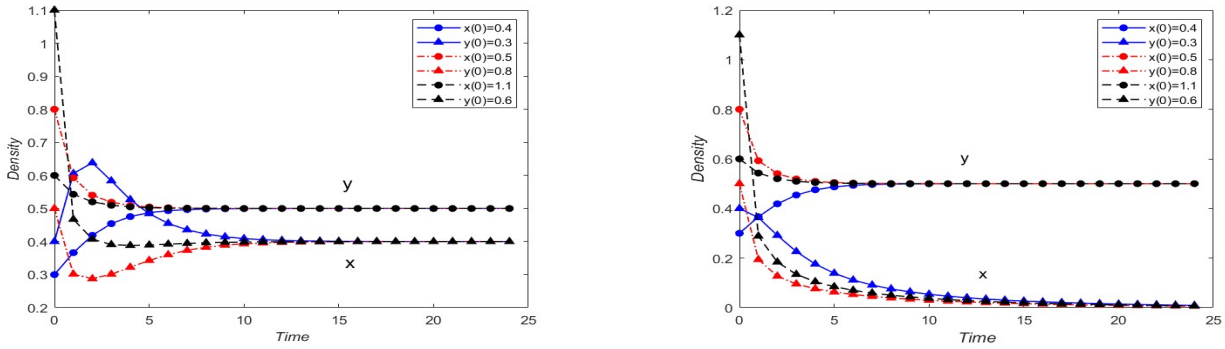

(a) $k = 2$ (b) $k = 4$

Figure 12. Global stability of positive equilibrium points E^* with $a_2 = 0.5$, e_2=1, $c = 0.2$, $e_1 = 3$.

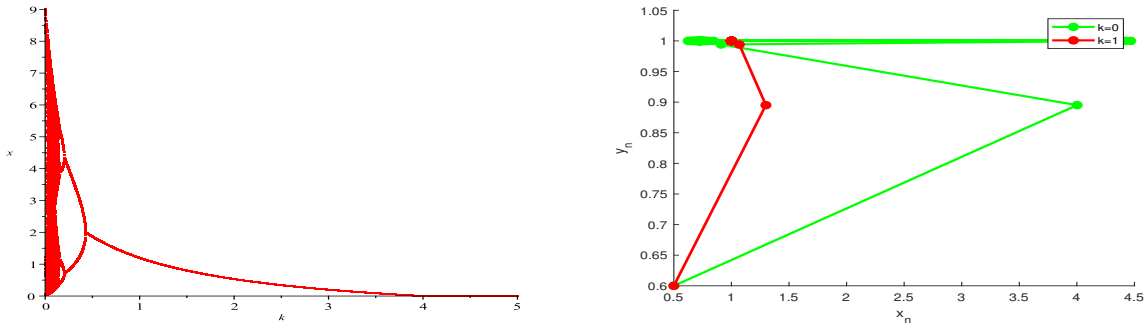

(a) (b) $k = 0, k = 1$

Figure 13. (a) Bifurcation graph with k as bifurcation parameter; (b) density trajectory plots of two species with different fear effect coefficients.

Additionally, examining the two trajectories shown in Figure 13(b) with $k = 0$ and $k = 1$ makes it clear that, as k increases, the solution approaches a stable state within shorter trajectories. This observation underscores the notion that an appropriate level of fear might confer advantages to species, enabling them to acclimate more effectively to changes in the surrounding environment.

Example 4. *(Effect of fear effect on the stability of the system)*

We proceed to investigate the influence of the fear effect on the system through numerical simulations. The chosen parameter values for this analysis are $(e_1, a_2, e_2, c) = (2, 1, 0.3, 0.2)$. The density distribution of the first species, denoted as x, and the second species, denoted as y, for varying values of k is illustrated in Figure 14. In this analysis, we examine two scenarios: one where the system exhibits a fear effect ($k \neq 0$) and another where there is no fear effect ($k = 0$). Furthermore, we categorize the presence of the fear effect into several levels, specifically $k = 0.3, k = 0.5, k = 1, k = 3, k = 5$. It was observed that an increase in the fear effect parameter k reduced the density of the first species and had no effect on the second species. However, it enhances the local stability of the first species and diminishes the frequency of oscillations. As the intensity of fear increases, the local stability of the first species will diminish, resulting in the prolonged period required to attain equilibrium. Moreover,

a higher value of k leads to the extinction of the first species.

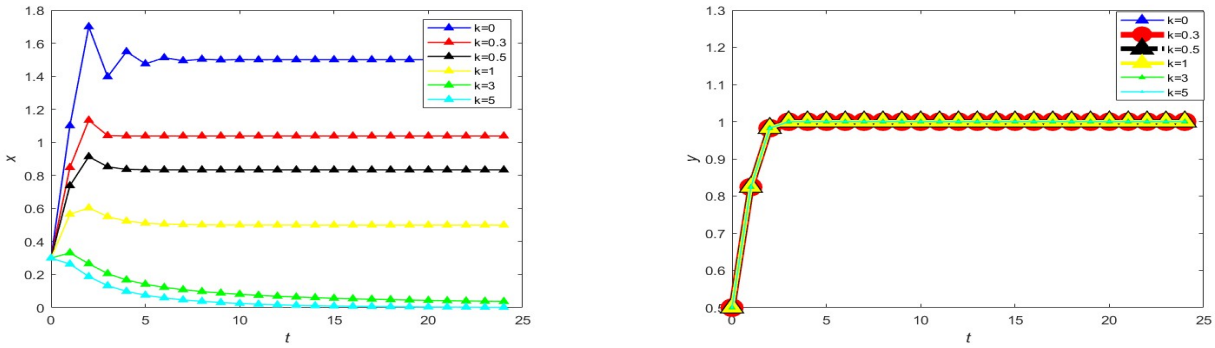

(a) x species densities. (b) y species densities.

Figure 14. The fear effect on the impact of the system (1.5) with $e_1 = 2$, $a_2 = 1$, $e_2 = 0.3$, $c = 0.2$.

Example 5. *The bifurcation parameter for the chaotic region is denoted as k, while the remaining parameter values are established as follows: the values of the variables* (e_1, a_2, e_2, c) *are as follows:* $e_1 = 4.3$, $a_2 = 1$, $e_2 = 0.3$, $c = 0.2$, *the given system, denoted as Eq* (3.7), *can be expressed as:*

$$\begin{cases} x_{n+1} = \rho x_n \exp\left(\dfrac{4}{1+ky_n} - 0.3x_n - 0.2y_n\right) + (1-\rho)x_n, \\ y_{n+1} = \rho y_n \exp\left(1 - y_n\right) + (1-\rho)y_n. \end{cases} \tag{4.1}$$

Based on the observation of Figure 7, it is evident that for values of k within the range of $0 < k < 0.5$, *the first species undergoes a chaotic state. Therefore, we select certain values of k such as* $k = 0.20, 0.25, 0.30, 0.35, 0.40, 0.45$. *By utilizing Theorem 3.3, in conjunction with Table 2, we can determine the range of values for* ρ *when* $0.2 \leq k \leq 0.5$.

Figure 15(a),(b) show that chaos control is effective.

Table 2. In the control system, the range of ρ corresponds to different k values.

Values of bifurcation parameter k from the chaotic region	**Stability interval** ρ
0.20	$0 < \rho < 0.648648648648$
0.25	$0 < \rho < 0.680272108843$
0.30	$0 < \rho < 0.712328767123$
0.35	$0 < \rho < 0.744827586206$
0.40	$0 < \rho < 0.777777777777$
0.45	$0 < \rho < 0.811188811188$

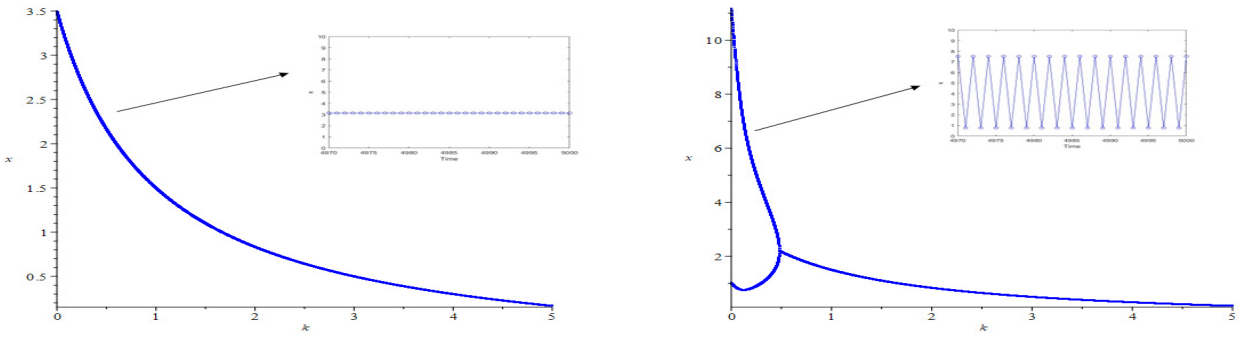

(a) The bifurcation plot of x when $\rho = 0.51$.

(b) The bifurcation plot of x when $\rho = 0.91$.

Figure 15. Bifurcation diagrams for controlled system (4.1) with $e_1 = 4.3$, $a_2 = 1$, $e_2 = 0.3$, $c = 0.2$.

5. Summary and discussion

Through numerical simulations, we find that when the fear effect k changes, the dynamic behaviors of the system will also change accordingly. We summarize the impact of the fear effect k on the system in Table 3:

Table 3. The impact of fear effect k on system dynamics behavior.

Conditions		**Case**
$0 < a_2 < 2$	$k > k^*$	The first species became extinct.
		As k increases, the density of the first species decreases.
	$k^{**} < k < k^*$	When the first species is in chaos, k has a stabilizing effect.
$a_2 > 2$	$k > k^*$	The first species became extinct.
	$0 < k < k^*$	Decrease in the density of the first species.

Additionally, through numerical simulations, we have observed some intuitively understandable phenomena:

1) Compared with the model (1.1) studied by Sun [9], considering the discrete amensalism model (1.5) with fear effect on the first species, the stability of the positive equilibrium point in model (1.5) changes, and the dynamic behavior will become more complicated. For example, transcritical bifurcation and flip bifurcation appear.
2) Compared to system (1.2), the trajectory of system (1.5) reaches its stable steady-state solution more rapidly as the fear effect increases. However, the first species will go extinct more quickly with an increasing fear effect.
3) The dynamic behavior of system (1.5) is different from that of system (1.2). For example, there is a flip bifurcation at the boundary equilibrium point and the positive equilibrium point, but there is also a transcritical bifurcation at $E_0(0, 0)$, which is not seen in system (1.2). The presence of a

transcritical bifurcation indicates that system (1.5) has some plasticity and adaptability to change from one stable state to another in the face of external changes or stresses. This adaptability helps species adapt more quickly to changes in their environment.

4) Zhou [21] did not study the global attractivity of the boundary equilibrium point of system (1.2). However, we notice that the boundary equilibria of system (1.5) is also globally attractive and its attractivity depends on the fear effect k, which means that the second species is stable and the extinction of the first species depends on the fear effect.
5) By observing Figure 1, Xi et al. [2] can only conclude that the fear effect will reduce the density of species. However, they have not conducted in-depth research on how the fear effect will be affected if it gradually increases. Through numerical simulation, it is not difficult to find if the fear effect is large enough to cause the extinction of the first species.

Finally, we must point out that an appropriate model usually takes functional responses into account, and the recent paper [18] explored the dynamical behavior of amensalism system with Beddington-DeAngelies functional response. However, no scholars have yet explored the influence of the fear effect on the dynamical behavior of amensalism system with Beddington-DeAngelies functional response, which will be further investigated in our subsequent work.

Use of AI tools declaration

The authors declare that they have not used artificial intelligence tools in the creation of this article.

Acknowledgments

The authors would like to thank four anonymous reviewers for their valuable comments, which greatly improved the final expression of the paper.

Conflict of interest

The authors declare that there is no conflict of interest.

References

1. J. P. Veiga, Commensalism, amensalism, and synnecrosis, *Encycl. Evol. Biol.*, (2016), 322–328. https://doi.org/10.1016/B978-0-12-800049-6.00189-X
2. X. Xi, J. N. Griffin, S. Sun, Grasshoppers amensalistically suppress caterpillar performance and enhance plant biomass in an alpine meadow, *Oikos*, **122** (2013), 1049–1057. https://doi.org/10.1111/j.1600-0706.2012.00126.x
3. C. García, M. Rendueles, M. Díaz, Microbial amensalism in Lactobacillus casei and Pseudomonas taetrolens mixed culture, *Bioprocess Biosyst. Eng.*, **40** (2017), 1111–1122. https://doi.org/10.1007/s00449-017-1773-3
4. J. P. Veiga, W. Wamiti, V. Polo, M. Muchai, Interphyletic relationships in the use of nesting cavities: Mutualism, competition and amensalism among hymenopterans and vertebrates, *Naturwissenschaften*, **100** (2013), 827–834. https://doi.org/10.1007/s00114-013-1082-x

5. J. M. Gómez, A. González-Megías, Asymmetrical interactions between ungulates and phytophagous insects: Being different matters, *Ecology*, **83** (2002), 203–211. https://doi.org/10.1890/0012-9658(2002)083[0203:AIBUAP]2.0.CO;2

6. Y. B. Hong, S. M. Chen, F. D. Chen, On the existence of positive periodic solution of an amensalism model with Beddington-DeAngelis functional response, *WSEAS Trans. Math.*, **21** (2022), 572-579. https://doi.org/10.37394/23206.2022.21.64

7. X. He, Z. Zhu, J. Chen, F. Chen, Dynamical analysis of a Lotka Volterra commensalism model with additive Allee effect, *Open Math.,* **20** (2022), 646–665. https://doi.org/10.1515/math-2022-0055

8. L. L. Xu, Y. L. Xue, Q. F. Lin, C. Q. Lei, Global attractivity of symbiotic model of commensalism in four populations with Michaelis-Menten type harvesting in the first commensal populations, *Axioms*, **11** (2022), 337. https://doi.org/10.3390/axioms11070337

9. G. C. Sun, Qualitative analysis on two populations amensalism model, *J. Jiamusi Univ.*, **21** (2003), 283–286.

10. Z. F. Zhu, Y. A. Li, F. Xu, Mathematical analysis on commensalism Lotka-Volterra model of populations, *J. Chongqing Inst. Technol.*, **8** (2008), 100–101.

11. Z. Wei, Y. Xia, T. Zhang, Stability and bifurcation analysis of an amensalism model with weak Allee effect, *Qualitative Theory Dyn. Syst.*, **19** (2020). https://doi.org/10.1007/s12346-020-00341-0

12. D. Luo, Q. Wang, Global dynamics of a Holling-II amensalism system with nonlinear growth rate and Allee effect on the first species, *Int. J. Bifurcation Chaos*, **31** (2021), 2150050. https://doi.org/10.1142/S0218127421500504

13. D. Luo, Q. Wang, Global dynamics of a Beddington-DeAngelis amensalism system with weak Allee effect on the first specie, *Appl. Math. Comput.*, **408** (2021), 126368. https://doi.org/10.1016/j.amc.2021.126368

14. M. Zhao, Y. Du, Stability and bifurcation analysis of an amensalism system with Allee effect, *Adv. Differ. Equations*, **2020** (2020). https://doi.org/10.1186/s13662-020-02804-9

15. H. Liu, H. Yu, C. Dai, H. Deng, Dynamical analysis of an aquatic amensalism model with non-selective harvesting and Allee effect, *Math. Biosci. Eng.*, **18** (2021), 8857–8882. https://doi.org/10.3934/mbe.2021437

16. R. Wu, A two species amensalism model with non-monotonic functional response, *Commun. Math. Biol. Neurosci.*, **2016** (2016), 19. https://doi.org/10.28919/cmbn/2839

17. Y. B. Chong, S. M. Chen, F. D. Chen, On the existence of positive periodic solution of an amensalism model with Beddington-DeAngelis functional response, *WSEAS Trans. Math.*, **21** (2022), 572–579. https://doi.org/10.37394/23206.2022.21.64

18. X. Guan, F, Chen, Dynamical analysis of a two species amensalism model with Beddington-DeAngelis functional response and Allee effect on the second species, *Nonlinear Anal. Real World Appl.*, **48** (2019), 71–93. https://doi.org/10.1016/j.nonrwa.2019.01.002

19. Y. Liu, L. Zhao, X. Huang, H. Deng, Stability and bifurcation analysis of two species amensalism model with Michaelis-Menten type harvesting and a cover for the first species, *Adv. Differ. Equations*, **2018** (2018). https://doi.org/10.1186/s13662-018-1752-2
20. M. Zhao, Y. Ma, Y. Du, Global dynamics of an amensalism system with Michaelis-Menten type harvesting, *Electron. Res. Arch.*, **31** (2022), 549–574. https://doi.org/10.3934/era.2023027
21. Q. Zhou, F. Chen, S. Lin, Complex dynamics analysis of a discrete amensalism system with a cover for the first species, *Axioms*, **11** (2022), 365. https://doi.org/10.3390/axioms11080365
22. C. Lei, Dynamic behaviors of a stage structure amensalism system with a cover for the first species, *Adv. Differ. Equations*, **2018** (2018). https://doi.org/10.1186/s13662-018-1729-1
23. Y. Liu, L. Zhao, X. Huang, H. Deng, Stability and bifurcation analysis of two species amensalism model with Michaelis-Menten type harvesting and a cover for the first species, *Adv. Differ. Equations*, **2018** (2018). https://doi.org/10.1186/s13662-018-1752-2
24. X. D. Xie, F. D. Chen, M. X. He, Dynamic behaviors of two species amensalism model with a cover for the first species, *J. Math. Comput. Sci.*, **16** (2016), 395–401. http://dx.doi.org/10.22436/jmcs.016.03.09
25. L. Y. Zanette, A. F. White, M. C. Allen, M. Clinchy, Perceived predation risk reduces the number of offspring songbirds produce per year, *Science*, **334** (2011), 1398–1401. https://doi.org/10.1126/science.1210908
26. K. H. Elliott, G. S. Betini, D. R. Norris, Experimental evidence for within- and cross-seasona effects of fear on survival and reproduction, *J. Anim. Ecol.*, **85** (2010), 507–515. https://doi.org/10.1111/1365-2656.12487
27. X. Wang, L. Zanette, X. Zou, Modelling the fear effect in predator-prey interactions, *J. Math. Biol.*, **73** (2016), 1179–1204. https://doi.org/10.1007/s00285-016-0989-1
28. A. A. Thirthar, S. J. Majeed, M. A. Alqudah, P. Panja, T. Abdeljawad, Fear effect in a predator-prey model with additional food, prey refuge and harvesting on super predator, *Chaos Solitons Fractals*, **159** (2022), 112091. https://doi.org/10.1016/j.chaos.2022.112091
29. K. Sarkar, S. Khajanchi, Impact of fear effect on the growth of prey in a predator-prey interaction model, *Ecol. Complexity*, **42** (2020), 100826. https://doi.org/10.1016/j.ecocom.2020.100826
30. J. Chen, X. He, F. Chen, The influence of fear effect to a discrete-time predator-prey system with predator has other food resource, *Mathematics*, **9** (2021), 865. https://doi.org/10.3390/math9080865
31. D. L. Ogada, M. E. Gadd, R. S. Ostfeld, T. P. Young, F. Keesing, Impacts of large herbivorous mammals on bird diversity and abundance in an African savanna, *Oecologia*, **156** (2008), 387–397. https://doi.org/10.1007/s00442-008-0994-1
32. Q. Zhou, F. Chen, Dynamical analysis of a discrete amensalism system with the Beddington-DeAngelis functional response and Allee effect for the unaffected species, *Qualitative Theory Dyn. Syst.*, **22** (2023), 16. https://doi.org/10.1007/s12346-022-00716-5
33. P. Panday, N. Pal, S. Samanta, J. Chattopadhyay, A three species food chain model with fear induced trophic cascade, *Int. J. Appl. Comput. Math.*, **5** (2019), 1–26. https://doi.org/10.1007/s40819-019-0688-x

34. S. K. Sasmal, Y. Takeuchi, Dynamics of a predator-prey system with fear and group defense, *J. Math. Anal. Appl.*, **481** (2020), 123471. https://doi.org/10.1016/j.jmaa.2019.123471

35. H. Zhang, Y. Cai, S. Fu, W. Wang, Impact of the fear effect in a prey-predator model incorporating a prey refuge, *Appl. Math. Comput.*, **356** (2019), 328–337. https://doi.org/10.1016/j.amc.2019.03.034

36. H. Singh, J. Dhar, H. S. Bhatti, Discrete-time bifurcation behavior of a prey-predator system with generalized predator, *Adv. Differ. Equations*, **2015** (2015), 206. https://doi.org/10.1186/s13662-015-0546-z

37. R. Banerjee, P. Das, D. Mukherjee, Stability and permanence of a discrete-time two-prey one-predator system with Holling type-III functional response, *Chaos Solitons Fractals*, **117** (2018), 240–248. https://doi.org/10.1016/j.chaos.2018.10.032

38. Q. Din, Complexity and chaos control in a discrete-time prey-predator mode, *Commun. Nonlinear Sci. Numer. Simul.*, **49** (2018), 113–134. https://doi.org/10.1016/j.cnsns.2017.01.025

39. H. Jiang, T.D. Rogers, The discrete dynamics of symmetric competition in the plane, *J. Math. Biol.*, **25** (1978), 573–596. https://doi.org/10.1007/BF00275495

40. F. Chen, Permanence for the discrete mutualism model with time delays, *Math. Comput. Modell.*, **47** (2008), 431–435. https://doi.org/10.1016/j.mcm.2007.02.023

41. D. C. Liaw, Application of center manifold reduction to nonlinear system stabilization, *Appl. Math. Comput.*, **91** (1998), 243-258. https://doi.org/10.1016/S0096-3003(97)10021-2

42. S. Wiggins, *Introduction to Applied Nonlinear Dynamical Systems and Chaos*, Springer Science and Business Media, 2003.

43. C. Robinson, *Dynamical Systems: Stability, Symbolic Dynamics and Chaos*, CRC Press, 1998.

Appendix

Lemma 3 Let $f(u) = u\exp(\alpha - \beta u)$, where α and β are positive constants, then $f(u)$ is nondecreasing for $u \in (0, \frac{1}{\beta}]$.

Lemma 4 Assume that sequence $\{u_n\}$ satisfy $u_{n+1} = u_n \exp(\alpha - \beta u_n)$, $n \in \mathbb{N}$, where α and β are positive constants and $u(0) > 0$. Then

(i) if $\alpha < 2$, then $\lim_{n\to+\infty} u(n) = \frac{\alpha}{\beta}$.

(ii) if $\alpha \leq 1$, then $u(n) \leq \frac{1}{\beta}, n = 2, 3, ...$

Lemma 5 Suppose that function $f,\ g : \mathbb{Z}_+ \times [0, +\infty) \to [0, +\infty)$ satisfy $f(n, x) \leq g(n, x)$ $(f(n, x) \geq g(n, x))$ for $n \in \mathbb{Z}_+$ and $x \in [0, +\infty)$ and $g(n, x)$ is nondecreasing with respect to x. If $\{x(n)\}$ and $\{u(n)\}$ are the solutions of the following difference equations

$$x(n + 1) = f(n, x(n)),\ u(n + 1) = g(n, u(n)),$$

respectively, and $x(0) \leq u(0)$ $(x(0) \geq u(0))$, then

$$x(n) \leq u(n)\ (x(n) \geq u(n)),\ \forall n \geq 0.$$

Lemma 2.1 Assume that $\{x(k)\}$ satisfies $x(k) > 0$ and

$$x(k+1) \leq x(k)\exp\left[a(k) - b(k)x(k)\right],\ k \in \mathbb{N},$$

where $a(k)$ and $b(k)$ are non-negative sequences bounded above and below by positive constants. Then

$$\limsup_{k\to+\infty} x(k) \leq \frac{\exp(a^u - 1)}{b^l},$$

where $a^u = sup_{n\in\mathbb{N}}\{a(n)\}, b^l = inf_{n\in\mathbb{N}}\{b(n)\}$.

Lemma 2.2 Assume that $\{x(k)\}$ satisfies

$$x(k+1) \geq x(k)\exp\left[a(k) - b(k)x(k)\right], k \geq N_0,$$

$\limsup_{k\to+\infty} x(n) \leq x^*$, and $x(N_0) > 0$, where $a(k)$ and $b(k)$ are non-negative sequences bounded above and below by positive constants and $N_0 \in N$. Then

$$\liminf_{n\to+\infty} x(n) \geq \min\left\{\frac{a^l}{b^u}\exp\left(a^l - b^u x^*\right), \frac{a^l}{b^u}\right\},$$

where $a^l = inf_{n\in\mathbb{N}}\{a(n)\}, b^u = sup_{n\in\mathbb{N}}\{b(n)\}$.

AIMS Press